BioTag: Robust RFID-based Continuous User Verification Using Physiological Features from Respiration

Bin Hu*, Tianming Zhao†, Yan Wang†, Jerry Cheng§, Richard Howard*, Yingying Chen*, Hao Wan§
*Rutgers University, †Temple University, §New York Institute of Technology

ABSTRACT

For decades, one-time verification has been the standard for user verification at entry points, office rooms, etc. However, such approaches request users to provide their secrets (e.g., entering passwords and collecting fingerprints) and re-verify (e.g., screen shutdown) manually. Thus, they cannot confirm whether the user is a legitimate or an imposter after verification, which raises the urgent demand for a more convenient and secure solution to perform continuous user verification. However, existing continuous verification methods heavily rely on users' active participation, which is inconvenient. Toward this end, we propose a continuous user verification system, BioTag, which utilizes the low-cost radio frequency identification (RFID) technology to capture unique physiological characteristics rooted in the users' respiration motions for continuous user verification. Specifically, we use two RFID tags attached to a user's chest and abdomen to capture the user's intrinsic respiratory patterns via RFID signals. We develop respiratory feature extraction methods based on waveform morphology analysis and fuzzy wavelet transformation (FWPT) to derive unique biometric information from the user's respiration signals. Furthermore, we develop an adaptive classifier using the gradient boosting decision tree (GBDT) to identify legitimate users and attackers accurately. Extensive experiments involving 41 participants demonstrate that BioTag can robustly authenticate users and detect various types of adversaries with low training effort. In particular, our system can achieve over 95.2% and 94.8% verification accuracy on random attack and imitation attack scenarios, respectively.

CCS CONCEPTS

• **Security and privacy** → **Authentication**.

KEYWORDS

vital signs, RFID, continues verification, respiratory pattern

ACM Reference Format:
Bin Hu*, Tianming Zhao†, Yan Wang†, Jerry Cheng§, Richard Howard*, Yingying Chen*, Hao Wan§. 2022. BioTag: Robust RFID-based Continuous User Verification Using Physiological Features from Respiration. In *The Twenty-third International Symposium on Theory, Algorithmic Foundations, and Protocol Design for Mobile Networks and Mobile Computing (MobiHoc '22), October 17–20, 2022, Seoul, Republic of Korea.* ACM, New York, NY, USA, 10 pages. https://doi.org/10.1145/3492866.3549718

MobiHoc '22, October 17–20, 2022, Seoul, Republic of Korea

ACM ISBN 978-1-4503-9165-8/22/10…$15.00
https://doi.org/10.1145/3492866.3549718

1 INTRODUCTION

Traditional one-time verification methods request a user to provide his/her credentials (e.g., password or fingerprint) during each verification process. Such practices are inconvenient and flawed from security perspectives. For instance, the user may need to re-repeatedly provide the password every time after screen shutdown, which is tedious and annoying. The more serious problem is that the credentials of the legitimate are vulnerable to many attacks (e.g., shoulder surfing attack [12] and smudge attack [2]), which make the one-time verification system compromisable. Recently, continuous user verification has attracted much attention due to its capability of periodically verifying the user's identity without active user inputs. As a result, it has shown a great potential to act as a second verification factor to the one-time verification and address its concerns.

Existing continuous verification approaches can be categorized into two categories (i.e., behavioral-based and physiological-based). Behavioral-based continuous verification leverages the specific human physical behaviors, such as gait pattern [34], keystroke [25], and hand gestures [15] to identify the user. Although these studies enable continuous user verification, they rely on users' active participation, which is intrusive and inconvenient in reality. Unlike behavioral-based approaches, physiological-based approaches could leverage always-exist vital signs to perform non-intrusive user verification continuously. Researchers have leveraged the cardiac biometrics [13], speech characteristics [33], and respiratory patterns [14] to perform continuous user verification. However, all these existing approaches require dedicated devices or users' active participation, which are not applicable in many practical scenarios. Unlike the existing work, Liu et al. [14] proposed a continuous verification system to capture the respiratory patterns by leveraging WiFi technology. Although the WiFi-based approaches do not require users to wear any devices, they cannot provide adequate user authentication for multiple users simultaneously. RFID technology has been proposed to enable passive breathing rate monitoring [19, 35] and user verfication with low costs. RF badge [19] adopts a badge with 4 tags to verify the user by capturing vital signs from the chest. However, it is not applicable to the users using abdominal breathing [26] and it is hard to keep the badge in the designated location and angle to capture stable RFID signals.

In this work, we devise an innovative RFID-based continuous verification system, BioTag, based on respiratory biometrics independent of any specific activities. BioTag leverages two low-RFID tags in a user's chest and abdomen areas to track the user's unique respiratory body movements (e.g., chest, abdomen, thoracic and diaphragm movements) by using the phase dynamics in the radio

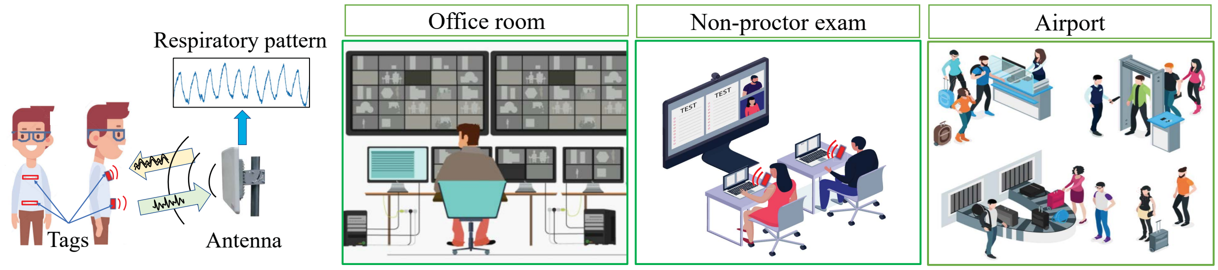

(a) Illustration of working flow **(b) Illustrations of applications**

Figure 1: Deployment of our system and example applications of continuous user verification that leverages respiratory motions captured by off-the-shelf RFID.

frequency signals backscattered from the tags. Different from existing works, users just need to wear the clothes with two passive RFID tags embedded at the chest and abdomen, which is more convenient than existing methods. Furthermore, the two tags attached to the abdomen and chest can comprehensively capture the fine-grained respiratory features caused by the respiratory motions of the different parts of the human body. As a result, BioTag achieves high verification accuracy on different people using different breathing styles with only a few training costs. In addition, our approach can verify multiple users simultaneously without performance reduction. Our system targets the professionals at different workplaces who demand convenient user verification and are willing to provide their identities in their work or business. For example, In a non-proctor exam scenario, our system can keep verifying examinees after they present their ID documents and enter the examination venue. Our system can also keep verifying the identities of ground staff and administrators after verifying their identities using fingerprints at the airport security checkpoint. Figure 1 illustrates the basic idea and real-world application scenarios of our system.

There are many challenges in realizing such non-intrusive continuous user verification using RFID in real-world scenarios. First, people have different breathing styles (e.g., breathe with the chest, breathe with the abdomen, or both), which results in difficulty locating the optimal tag location for capturing the clear respiratory signals of various people. Second, the human dynamics caused by respiratory motions are very subtle and easily interfered with by many factors in real environments. It is non-trivial to determine features from RFID signals that are robust and effective for capturing users' unique respiratory characteristics. Third, human respiratory patterns could drift slightly on different days [24] which leads to the changes in the RFID waveform pattern and potentially impact the performance of user verification.

To address these challenges, we first conducted an extensive preliminary study and finalized two tags attaching locations as chest and abdomen. Specifically, these two locations are chosen to guarantee a clear respiratory pattern being captured for different breathing ways. We investigate and determine to use waveform morphology analysis and fuzzy wavelet packet transform (FWPT) [11] to capture unique characteristics of respiratory motions for continuous verification. Moreover, our system adopts an adaptive updating mechanism to automatically accommodate the user's respiratory signal changes over time based on adaptive training of associated classifiers. The main contributions of our work are summarized as follows:

- The system can utilize RFID tags attached to users' clothes to capture the unique respiratory patterns without requiring active user participation.
- We perform a comprehensive study to determine the best position on human bodies to capture users' respiratory patterns using RFID tags. Our study demonstrates that two tags attached to the chest and abdomen are sufficient to derive unique respiratory characteristics for accurate user verification verification.
- We develop new respiratory features that can effectively extract unique user biometric information through fiducial-based analysis and fuzzy-wavelet-packet-based analysis. We also develop an adaptive learning-based classifier to ensure robust continuous user verification under different attacks.
- Our extensive experiments involve 41 volunteers and different setups of RFID devices and attack models. The results demonstrate that our system can achieve over 94.8% verification accuracy while robustly detecting various types of attacks and less than 3.9% false-positive rate.

2 RELATED WORK

Existing studies have shown that vital signs (i.e., heartbeat and respiration) can be used for identifying users. For instance, electrocardiogram (ECG) [21], photoplethysmography (PPG) [9], and cardiac motions [13] have been employed to identify users. BreathPrint [5] has exploited the breathing sound for user verification. However, these approaches require users to either attach sensors to their body or use dedicated sensors that are not readily available in the commodity devices.

WiFi-based sensing has attracted considerable attention from many researchers due to the prevalence of wireless signals in indoor environments. Channel state information (CSI) has been proposed to capture human behaviors, such as gait patterns [34], and activities [28] to perform user verification. These approaches can only verify users when they perform activities that are not always available in practice. Few works leverage WiFi to capture vital signs for user verification. For instance, Liu et al. [14] can identify users by extracting respiration related signals from CSI. Although it does not require users to perform activities, WiFi is not scalable in multi-user scenarios.

Recently, RFID signals have been exploited for vital signs monitoring. For example, Zhang *et al.* [35] attach tags on the front and back of the abdomen and extract users breathing rate in moving scenarios. TagBreathe [29] places three tags on the chest, lower

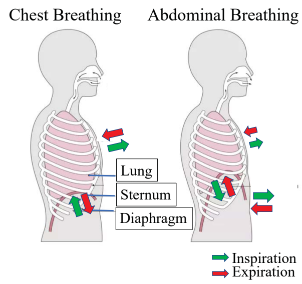

(a) Illustration of chest breathing and abdominal breathing

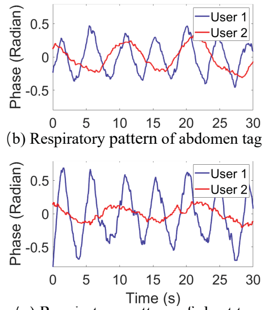

(b) Respiratory pattern of abdomen tag

(c) Respiratory pattern of chest tag

Figure 2: Distinct respiratory patterns captured by RFID measurements.

abdomen, and in between to improve the breathing rate monitoring accuracy. RF-ECG [27] extracts heartbeat rates from RFID signals of a tag array attached to the chest area in the clothes. However, these works only design a one-dimension feature to estimate the respiratory rate, which is not comprehensive enough to capture the unique respiratory characteristics for user verification. In the security domain, Au-Id [7] can identify users based on their daily activities captured by RFID signals. However, it needs users to perform a specific activity, which is not applicable for some scenarios. RFace [31] proposes to perform one-time user verification by extracting the 3D geometry and inner biomaterial features of faces using an RFID tag array. More recently, RF-badge [19] designs a badge with 4 tags to capture users' vital signs from the chest for user verification. However, RF-badge is not practical in use because the user is hard to keep the badge in the designated location and angle to capture stable RFID signals, which may introduce significant errors. Different from existing work, we leverage two low-cost RFID tags that can be embedded into users' clothes to comprehensively track users' unique physiological characteristics rooted in respiratory motions in the chest and abdomen in addition to respiration rates to perform user verification. It is more robust to environmental noise and can support multi-user verification simultaneously.

3 APPROACH OVERVIEW

3.1 Attack Model

In this work, we assume that attackers cannot compromise the hardware and software of the proposed continuous verification system (e.g., damage the RFID reader/antenna, block the communication between tags and the reader, damage or modify raw RFID measurement, gain access to memory storage of the continuous verification process, or have any knowledge of the trained machine learning model). We focus on the verification of the RFID measurements. An attacker is trying to fool and pass the verification system. Based on this, we consider the impact of two different types of attacks to evaluate the effectiveness of the proposed scheme as follows:

Random Attack. The attacker does not know the respiratory pattern of a target user. When attacking the system, the attacker stays in the same position as the target user and breathes in a normal way in terms of the breathing rate, inspiration/expiration rhythm, and depth.

Imitation Attack. The attacker first observes the legitimate user's respiration process to capture the respiratory patterns, including breathing rates, inspiration/expiration rhythms, and breathing depths. Then the attacker imitate the legitimate user's respiratory pattern to pass the verification system.

(a) **Tags on different locations (only 2 tags at a time)**

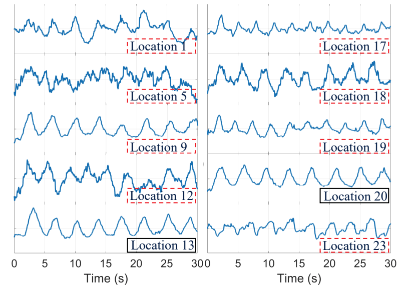

(b) **Respiratory patterns of different locations**

Figure 3: Illustration of placement study on different body locations and representative RFID measurements.

3.2 Feasibility Study

When a human breathes, the human respiration process includes inspiration and expiration stages that involve complex body movements. There are two types of breathing [26] causing different patterns in body movements: chest breathing and abdominal breathing, as illustrated in Figure 2a. The chest breathing is characterized by an upward and outward movement of the chest, where the sternum and diaphragm move up and down. The abdominal breathing involves little chest movements, and the sternum and diaphragm have a reverse movement trend. Due to the complex and diverse physiological structures of human body, the respiratory movements related to chest, abdomen, or other part of human body will show different amplitudes and patterns from person to person. Existing studies [20] have demonstrated that human respiratory movement has unique biological characteristics. Moreover, respiratory motions usually remain stable for a long time despite the variations in ages, smoking habits, weights, and whether having mild respiratory diseases [22]. These studies confirm that respiratory patterns can be a good biometric for continuous user verification.

Recently, researchers and manufacturers started to embed low-cost passive RFID tags into fabrics to achieve non-intrusive, cost-effective healthcare monitoring [1]. Existing works [33, 35]have shown that phase information in the backscattered signals from RFID tags can be leveraged to monitor breathing rates. Given the distance between the reader antenna and the tag is d, the RFID reader outputs a phase value θ of the backscatter radio wave from the tag as follows:

$$\theta = (\frac{2\pi}{\lambda} \times 2d + c) \bmod 2\pi, \tag{1}$$

where λ is the wavelength, and c is a constant phase offset that captures the influence of reader and tag circuits independent of the distance between the reader antenna and the tag. Equation 1 shows that θ is a function d. When the tag is attached to the human body, d changes periodically following the chest and abdomen movements when the person is breathing. Since most of the commercial off-the-shelf RFID readers can report the received phase values with a resolution of $2\pi/4096 \approx 0.0015$ radians, RFID technology can differentiate small changes in d with a resolution of 0.0038mm [33, 35], which is good enough to capture the minute body movements caused by respiration.

To demonstrate the feasibility of using RFID to capture respiratory patterns for user verification, we conduct experiments by attaching RFID tags to the chests and abdomens of two volunteers (i.e., user 1 and user 2) sitting in front of the RFID antenna and breathing normally. Figure 2b and 2c show the phase values after filtering the noises. We observe that the respiratory patterns corresponding to the two volunteers are significantly different in terms of morphological characteristics, such as pulse width, pulse amplitude, pulse shape, and small fluctuations around the wave peak/trough in the figure. We also observe that two people use different breathing styles resulting in distinct chest and abdomen respiratory patterns. For instance, the phase of the chest is greater than the abdomen for user 1 and opposite for user 2.

Placement Study. When human breaths, the movements of the chest, abdomen, and nearby body parts generate breathing signals. To increase the robustness and performance of the proposed verification system, we need to find the optimal body locations that can generate clear, strong, and stable respiratory patterns. To the best of our knowledge, none of the existing works studies this issue. Towards this end, we conduct a preliminary study in placing tags on 24 different body locations to find the optimal ones (Figure 3a). Figure 3b shows the corresponding RFID measurements in some representative locations. We observe that we could get a clear and stable respiratory pattern from 3 locations (i.e., locations 9, 13 and 20) at the middle chest and upper abdomen. The locations in the neck (i.e., locations 1 to 3), upper chest (e.g., locations 4 to 8), lower chest (i.e., locations 14 to 18), and middle abdomen (i.e., locations 22 to 24) are not suitable to use. We also observe that the RFID patterns (e.g., locations 9 and 13) show strong symmetry relative to the vertical center line of the human body. Therefore, we choose Locations 13 and 20 to deploy tags in our system.

3.3 System Overview

The basic idea of our system is to capture the unique physiological characteristics inherited from the human respiration process for continuous user verification leveraging RFID signals. The architecture of the proposed system is illustrated in Figure 4. The BioTag first collects time-series RFID phase measurements from two RFID tags attached to the chest and abdomen and applies *Phase Calibration* to calibrate the raw phases of different channels to the same channel. The calibrated phase data is then processed to remove the baseline drifts and high-frequency interferences via *Noise Removing* (i.e., low-pass and Kalman filters). Then, we utilize the *Interpolation* to resample the phase sequence with a uniformed sampling rate since the RFID reading uses a different sampling rate in each trial. To obtain the most reliable respiratory signals, the BioTag leverages the threshold-based *Movement Mitigation* to avoid the impact of large body movements.

Then, the system performs the *Respiration Segmentation* to determine each segment of RFID measurements containing a full respiratory trough-crest-trough pattern by identifying the increasing and decreasing trends (i.e., an up-down pattern) from the inspiration and expiration processes. After extracting each respiratory segment containing an entire inspiration and expiration process, we employ a Dynamic Time Warping (DTW) [18] algorithm to remove the outliers containing the irregular respiratory patterns, and then develop a new feature extraction mechanism adopting *Fiducial features* and *FWPT features* to describe the unique fine-grained biometric information rooted in respiratory motions comprehensively. The Fiducial features focus on the shapes of the respiration-related RFID patterns and capture the physiological characteristics of respiratory motions (i.e., respiration depths and durations in different breathing stages). The FWPT features analyze the respiration segment in the frequency domain using the wavelets in different scales, generating more fine-grained features that can reflect the complicated frequency characteristics of respiratory motions. Unlike the existing studies that fuse the respiratory patterns from different tags into one pattern and lose some essential biometric information from different body locations (e.g., chest and abdomen), our approach keeps these respiration features of each tag as a unique footprint to differentiate users.

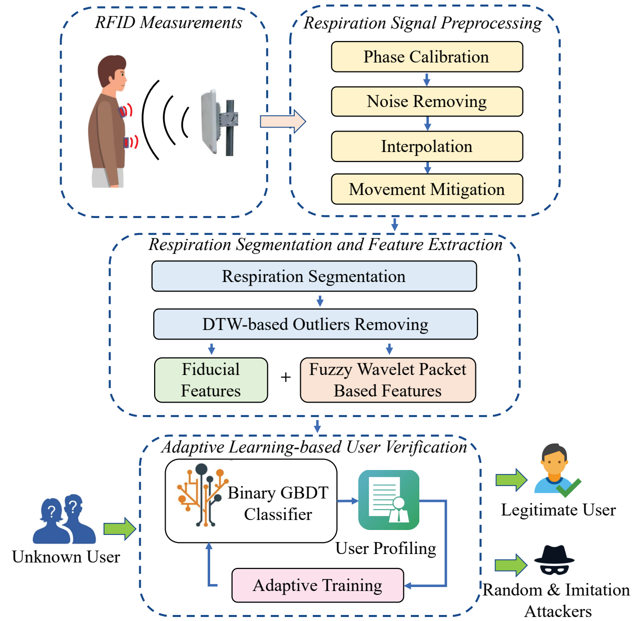

Figure 4: System architecture.

During the user enrollment phase, we construct a user's profiling based on the extracted features and use Gradient Boosting Decision Tree (GBDT) [6] in training the classifier. Our system can recognize the legitimate user's identity by the trained classifier and defend against various attacks (i.e., random attacks or imitation attacks). If the user's breathing pattern has a slight change due to strenuous exercises or fluctuating emotions, our system is designed to perform *Adaptive Training* with new training data to accommodate the changes.

During the verification phase, our system collects respiration segments in real-time and determines whether a current user is a legitimate user or not. Specifically, our system takes the extracted intrinsic physiological features of the incoming respiration segments as the input to perform the *Adaptive Learning-based User Verification* by using the binary GBDT classifier with trained user profiling. Finally, our system utilizes a majority-vote rule on the classified results of the T continues RFID segments to perform continuous verification.

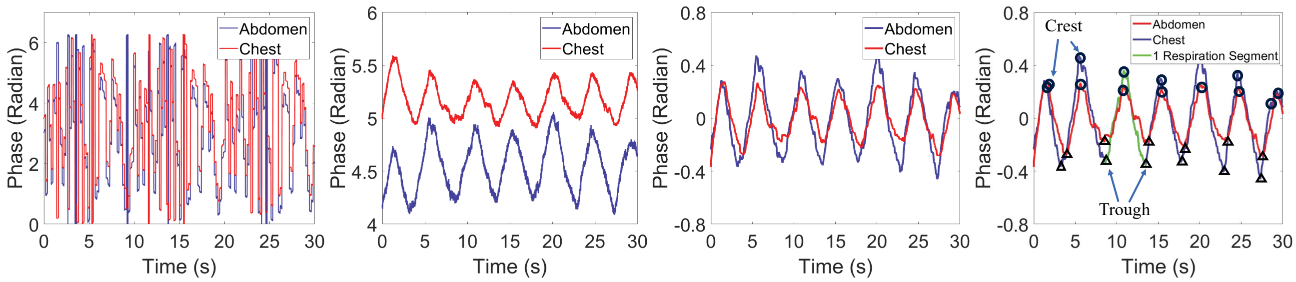

(a) Raw phase pattern (b) Calibrated phase pattern (c) Phase pattern after pre-processing (d) Respiration segmentation

Figure 5: Illustration of the phase calibration, filter, movement mitigation, and respiration segmentation process.

4 RESPIRATION SIGNAL ANALYSIS

4.1 Problem Formulation

We propose to leverage the RFID phase measurement θ on the distance d between the antenna and the RFID tag to capture the periodical signal of breathing caused by chest and abdomen movements. The RFID phase measurements θ can be modeled by the following equation:

$$\theta = (\frac{2\pi}{\lambda} \times 2d + \theta_T + \theta_R + \theta_{TAG} + \theta_{AIR}) \bmod 2\pi, \qquad (2)$$

where λ is the wavelength, d is the distance between antenna and tag, θ_T and θ_R are the phases introduced by the RFID reader's transmitting and receiving circuits, θ_{TAG} is the phase introduced by the tag's reflection characteristic, and θ_{AIR} is the phase introduced by the back-scattered channel. During a breathing cycle, d changes between a range of $[d_i, d_e]$ corresponding to the inspiration and expiration stages. Accordingly, we can derive θ_i and θ_e by replacing d in Equation 2 with d_i and d_e. Thus, the phase change $\Delta\theta$ caused by the user's respiration can be calculated as $\Delta\theta = \theta_i - \theta_e$. We find that the body movements caused by respiration are subtle, which causes little impact on the environment and multipath effects. Therefore, θ_T, θ_R, and θ_{AIR} in Equation 2 can be considered the same in θ_i and θ_e. In addition, θ_{TAG} is also the same since the RFID tags are the same. As such, $\Delta\theta$ can be simplified as:

$$\Delta\theta = (\frac{4\pi}{\lambda} \times (d_i - d_e)) \bmod 2\pi = (\frac{4\pi}{\lambda} \times \Delta d) \bmod 2\pi. \qquad (3)$$

Equation 3 shows that, by using the difference between θ_i and θ_e, we can eliminate the impacts of phase disturbances from environments, circuits, and tags and enhance the signals caused by the user's respiration. We note that our system derives two phase change measurements based on the RFID signals from two tags attached to the user's chest and abdomen (i.e., $\Delta\theta_{chest}$ and $\Delta\theta_{abdomen}$) to capture unique respiratory characteristics for user verification comprehensively.

4.2 RFID Data Preprocessing

The FCC regulation requires frequency hopping for UHF RFID systems. Thus, the phase offset generated by frequency hopping should be firstly removed in the signal pre-processing. We follow the existing calibration method [17] to restore the correct phase value on raw RFID measurements. The calibrated RFID measurements contain baseline drifts and high-frequency interferences. Therefore, BioTag performs the Noise Removing to reduce such impacts. We first apply a low-pass filter (0.5Hz) on the calibrated signal to reduce the high-frequency noise since the standard human breathing rate is lower than 0.5Hz. Moreover, as the phase noises of RFID measurements follow the Gaussian distribution [33], we design a Kalman filter [30] to reduce the ambient noises but keep the signals caused by the respiration. In addition, our system (i.e., Impinj R40 reader) adopts a frame slotted Aloha protocol to interrogate the tags randomly based on the EPC Gen2 standard [23], which makes the uniform sampling over the tags impossible (i.e., 180Hz - 200Hz for 2 tags). To tackle this issue, we use a cubic spline interpolation method [16] to re-sample the phase sequence with a uniform sampling rate (i.e., 220Hz) based on the assumption that the phase sequences change continuously. Comparing Figure 5a and Figure 5b, we can see that the calibrated phase data exhibits an obvious breathing signal, which is in great contrast to the raw phase data with the frequency hopping offsets.

4.3 Regular Body Movement Mitigation

The respiratory motions are much smaller compared to large body movements (e.g., standing up, walking, and shrugging). Therefore, the relatively weak respiratory pattern will be submerged in large motion patterns. To avoid the impacts of large body movements, we leverage a threshold-based method [32] to remove signals with apparent fluctuations due to the large body movements and focus on stable repetitive signals. We use φ to denote the sum of mean absolute deviations (MAD) of phase values for two RFID tags in a sliding window, as shown in the following equation:

$$\varphi = \frac{1}{|W|} \sum_{j=1}^{2} \sum_{k \in W} |\hbar^j(k) - m(\hbar^j(k))|, \qquad (4)$$

where W is the index set of all the packets in the sliding window, $|W|$ is the length of the sliding window, 2 is the number of RFID tags, $\hbar^j(k)$ is the phase for packet k from tag j and $m(\hbar^j(k))$ is the average value of $\hbar^j(k)$ in one sliding window. The insight of the method is that if the subject is moving, the phase will have larger variations (due to large changes in d). If the body movements duration is longer compared to one respiration cycle (i.e., $3-5$s) [3], the captured RFID measurement is too noisy for the fine-grained respiratory pattern. Therefore, we skip the RFID measurement for the long body movements (i.e., duration $>$ 1s) and mitigate the impaction of short body movements (i.e., duration $<$ 1s). Since the human body almost stays at the same position for a short body movement, we can remove the sudden big phase change by setting the window size as 6s and the threshold as 0.9 experimentally.

After detecting and excluding the RFID signals caused by large body movements, the signals still contain signal fluctuations caused by small body motions. Such signal fluctuations also cause phase shifts interfering with human respiration signals. We develop a Hampel filter with a windows size of 2000 and a threshold of 0.001

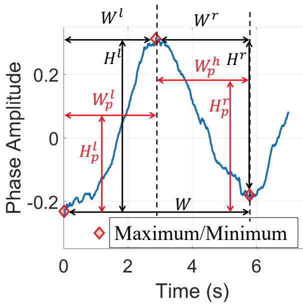

Feature	Description
W	Respiration Width
W^l	Left Width
W^r	Right Width
H^l	Left Height
H^r	Right Height
f_p^l	$f_p^l = W_p^l/H_p^l, p = 50, 100$
f_p^r	$f_p^r = W_p^r/H_p^r, p = 50, 100$

Figure 6: Illustration of fiducial features.

to remove all unrelated factors. Furthermore, our system adopts a detrending method [8] to remove the constant phase shift introduced by the random initial offset of the first channel before further processing. Figure 5c shows the pre-processed signal has a sufficiently clear and smooth repetitive pattern that can facilitate the respiration segmentation and feature extraction in the next step.

5 RESPIRATION-BASED USER VERIFICATION

5.1 Respiration Segmentation and Outliers Removing

We observe that filtered respiratory signals exhibit up-down patterns as shown in Figure 5c. Therefore, we define that a respiration segment starts from a trough and goes through a crest, which indicates the inspiration stage. Then the respiration segment ends at the second trough from the crest, which indicates the expiration stage. To identify the accurate positions for crests and troughs, we develop a *Crests/Troughs Points Selection* algorithm, which applies two thresholds (i.e., $Tmax$ and $Tmin$) to restrict the minimum distances between two neighboring crests or troughs, respectively. We adopt threshold 13 for $Tmax$ and 11 for $Tmin$ based on normal respiration rate (12 to 16 breaths per minute). Additionally, we also develop a *Fake Crests/Troughs Removing* algorithm, which iteratively removes the redundant crests between two troughs and redundant troughs between two crests. Figure 5d shows our segmentation method can effectively determine respiration segments. Moreover, we employ a Euclidean Distance-based DTW algorithm for respiratory outlier (i.e., generated by body movements and environmental noise) identification and removing. The basic idea is to leverage DTW distance between the outlier and regular respiratory segments to identify the outlier. Specifically, in the training phase, we derive a similarity index based on DTW distances among a few regular respiratory segments of the user. The similarity index between n respiration segments is defined as:

$$Index(V) = {}^1/_n \sum_{u=1}^{n} dtw(u, v), \tag{5}$$

where $u \in [1, n]$ and $v \in [1, n]$. In the testing phase, we calculate the DTW distances between each incoming segment. If the DTW distance exceeds the similarity index, we consider the incoming segment as an outlier.

5.2 Respiratory Feature Extraction

Fiducial Features. In order to obtain unique respiratory characteristics, we conduct multidimensional extraction of the fiducial characteristics to derive the 9 fiducial features that characterize representative patterns in each respiration segment of one tag's signal (e.g., chest or abdomen). Specifically, respiration width (W) represents the time duration of one respiration segment from left trough to right trough. left width (W^l) and right width (W^r) represents the time duration of one respiration segment from left trough to crest and crest to right trough. left height (H^l) and right height (H^r) is the difference of the phase amplitude between the left and right trough and crest. Let f_p^l denote the ratio of time duration to amplitude difference for the inspiration segment: $f_p^l = W_p^l/H_p^l$, describing the relationship between the inspiration depth and inspiration time duration when a respiratory motion is finished $p\%$: let f_p^r denote the ratio of time duration to amplitude for the expiration segment: $f_p^r = W_p^r/H_p^r$, representing the relationship between the expiration depth and expiration time duration when an expiration motion is finished $p\%$. Based on 41 people's respiration data collected in this work, we empirically determine $p = 50, 100$ to compute the fiducial features f_p^l and f_p^r, respectively. A total of 9 fiducial features can then be obtained for each respiration segment for each tag as shown in Figure 6 . We find that these features are generally effective for user verification because they are connected to human respiration systems and are always available regardless of the source of the RFID measurements (i.e., either chests or abdomens). Since we have two tags on the chest and abdomen independently, we extract 18 fiducial features containing the unique physiological characteristics of respiratory patterns for different people with different breathing styles.

Fuzzy Wavelet Packet Features. In addition to the fiducial features, we perform FWPT on each respiratory segment to construct fine-grained respiratory features. FWPT decomposes approximation and detail subspaces of the raw respiratory segment to realize fine-grained multi-resolution (i.e., time-frequency) analysis. Therefore, FWPT can capture the distinct respiratory biometrics by analyzing the minuscule differences of respiratory movements and vibrations for different body parts in various frequency domains. Particularly, we perform 8 level fuzzy wavelet packet decompositions obtaining 511 wavelet subspaces as FWPT features for each respiration segment obtained from each tag.

To improve the uniqueness of the extracted features, we develop an intrinsic physiological feature that concatenates the fiducial and FWPT features extracted from the RFID tags on the chest and abdomen. We note that this feature retains the comprehensive biometric characteristics derived from independent respiratory motions of both chest and abdomen. In contrast with existing fusion studies that accumulate the maximum value of features from different tags, our approach keeps the essential biometric information captured by each tag as a unique footprint to identify users effectively.

5.3 Machine learning based User Verification

We develop a user verification module using GBDT. Compared to other machine learning methods (e.g., Random Forest, SVM, and Neural Network), GBDT has the advantage of providing higher accuracy with lower training cost, the flexibility of optimizing on different loss functions to handling mixed features with different scales, which is exactly the characteristic of the intrinsic physiological features [36]. Specifically, given N training samples $\{(x_i, y_i)\}$, where x_i and y_i represent the intrinsic physiological features set and the corresponding identity label of the user (i.e., $y_i = 1$ or 0 represents whether x_i is from a legitimate user or not), the objective

(a) Location of RFID tags (b) Experimental setup

Figure 7: Illustration of experimental setup.

of GBDT is to minimize the loss function as follows:

$$L = \sum_{i=1}^{N} l(y_i, \phi(x_i)), \tag{6}$$

where $\phi(\cdot)$ is a optimization fuction and $\phi(x_i) = \sum_{m=1}^{M} \omega_m \bar{\lambda}_m(x_i)$. GBDT aims to find a appropriate $\phi(\cdot)$ to minimize the loss function $l(\cdot)$ by selecting the optimal weak learners $\bar{\lambda}_m$ and weights ω_m.

We adopt the GBDT implementation from the Scikit-learn [4]. In order to optimize the speed and accuracy of the GBDT model, we empirically choose the loss function $l = e^{y_i \phi(x_i)}$ and use the following parameter set to train the GBDT classifier: number of estimators = 2000, learning rate = 0.01, max depth = 50, and subsampling = 0.6. During the training phase, we train a binary GBDT classifier for each legitimate user. In the verification, the system uses the trained binary classifiers to classify incoming respiration-related feature set x. We compute confidence scores from each binary classifier and select the output of the classifier generating the highest confidence score as the final user verification result.

Majority Voting and Adaptive Training. In this study, a majority voting mechanism that combines the results of multiple continuous segments is used to achieve high verification accuracy. Our system selects the classification result receiving more than half of the votes. Specifically, we consider T continuous RFID segments as a basic user verification unit. If half or more than half of the respiratory segments in a window are classified as the same legitimate user, the system determines that the legitimate user is verified. Otherwise, the user does not pass the user verification. This process can significantly reduce the verification errors and improve the robustness of our system. Unless mentioned elsewhere, T is 3 respiration segments, which generally provide good performance, as shown in our evaluation.

We observe that users' respiratory patterns may vary slightly on different days since their respirations may be influenced by various factors (e.g., health conditions, emotions, and body temperatures). Therefore, we employ an adaptive training mechanism to fine-tune the trained classifier based on recent RFID measurements. Specifically, we define the user verification success rate Ver_s as the number of successful verification events Eve_s over the total number of verification events Eve_t within a time window (e.g., 60 mins). Our system continuously performs user verification at a designated rate (e.g., 18 verification events per min) and derives the Ver_s for each user. When a user fails the user verification, the system asks the user to provide the credential (e.g., password) to confirm the identity and records it as a failure event Eve_f. Otherwise, the system records it as a Eve_s. When the Ver_s of the user is below a threshold (e.g., 90%), the system determines that the user's respiratory patterns have slightly changed and then re-trains the model to improve the system performance by adding a small portion of recently verified RFID data (e.g., *ten* segments) into training datasets.

6 PERFORMENCE EVALUATION

6.1 Experimental Methodology

Hardware and Software. We use a commodity RFID reader Impinj R420, equipped with a directional antenna Laird S9028PCL, to collect data from the RFID signals sent by Impinj E41-B tags. The RFID signals hop among 50 channels within a spectrum from 902.5MHz to 927.5MHz. We implement a user interface and a verification module on a Thinkpad laptop, which collects data (i.e, phases, and time stamps) from the RFID reader through the low-level reader protocol - LLRP.

Experimental Setups. We attach two RFID tags to a participant's clothes in the chest and abdomen areas as shown in Figure 7(a). During each experiment, a participant sits on a chair that is 1m in front of the antenna. We keep the antenna at the same height as the participant's chest as shown in Figure 7(b). Participants are asked to breath normally during the experiments. To evaluate our system's robustness in different environments, we conduct experiments in four types of indoor spaces including a bedroom with a twin-size bed (4.2m×4.3m), a typical lab with office furniture and (3.0m×5.0m), a corridor with no obstacle (2.8m×2.8m), and a home office with office furniture (7.0m×4.0m).

Data Collection. We conduct extensive experiments with 41 participants (i.e., 33 males and 8 females, aging from 12 to 70) for 3 days at different times across 5 months. Each participant take part in 10 experiments, each of which last 60s. We also collect about $200 - 300$ respiration segments for imitation attacks, treating 1 participant as a legitimate user and 15 participants as the attackers. Unless mentioned otherwise, we use 70% respiration segments of each legitimate participant for training and the rest of the segments for testing.

6.2 Evaluation Metrics

Our system periodically verifies users based on the specific RFID segments. We define our evaluation metrics as follows: 1) *verification accuracy* - the percentage of the decisions declaring legitimate users correctly; 2) *attack detection rate* (true positive rate) - the percentage of decisions declaring attackers correctly; 3) *attack false detection rate* (false positive rate) - the percentage of decisions incorrectly declaring attackers; 4) *receiver operating characteristics (ROC) curve* - showing the attack detection rates and attack false detection rates under different values of thresholds.

6.3 Performance of Continuous User Verification

We first evaluate the user verification accuracy under the random attack and the imitation attack scenarios with different numbers of respiration segments. Specifically, in the random attack scenario, we consider 11 of the 41 participants as legitimate users, and the other 30 act as attackers. In the imitation attack case, a particular user is selected to be legitimate and 14 other users act as attackers. Figure 8a illustrates the user verification accuracy under the random and imitation attack scenarios. We observe that under the random attack scenario, the average verification accuracy is over 93.8%

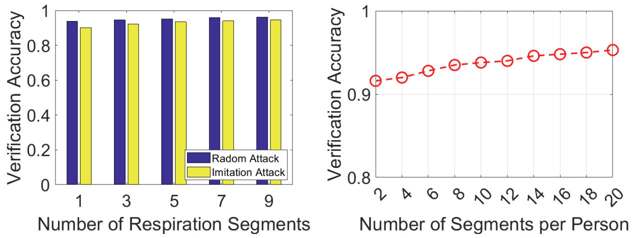

(a) Performance with different testing segments (b) Performance with different training sizes

Figure 8: Impacts of the defferent testing segments and training size.

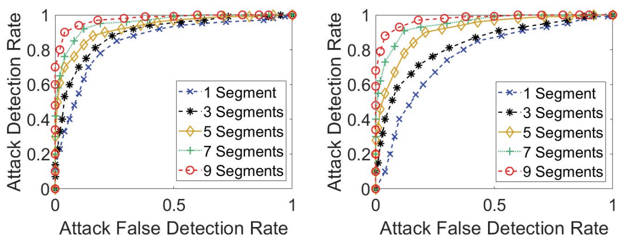

(a) ROC curves of random attack (b) ROC curves of imitation attack

Figure 9: ROC curves under random attack and imitation attacks.

when only one respiration segment is used. However, our system still achieves more than 95.2% verification accuracy when 3 or more respiration segments are used. Under the imitation attack, the average verification accuracy is around 90.4% using 1 respiration segment. The accuracy is lower is because a dedicated attacker is set to imitate legitimate users' respiratory patterns. However, the accuracy can still reach over 94.8% when 3 or more respiration segments are used. These results demonstrate that our system using commodity RFID devices is promising in practice.

Moreover, our system under the random attack scenario can achieve over 94.8% attack detection rate and less than 3.9% for attack false detection rate with 3 or more respiration segments. In addition, our system achieves over 92.1% attack detection rate and less than 4.2% attack false detection rate with 3 or more respiration segments under the imitation attack. Those results, which are shown in Figure 9a and Figure 9b, demonstrate that our system is robust against attack scenarios.

In addition, we examine the four additional machine learning models, SVM, neural network (neurons: 60-60-30), LeNet-5, and ResNet-50, as a comparison to the GBDT model, respectively. We observe that the GBDT achieves the best verification accuracy of 95.2% than other models, whose verification accuracies are 82.2%, 69.2%, 45.2%, 40.9% with 20 training and 3 testing segments, respectively. This result indicates that GBDT is easily tuned with a few training samples and is more suitable for our continuous verification system than the other machine learning methods.

6.4 Impact of Various Factors

Impact of Number of Testing Segments. We design a majority voting method that uses a 1,3,5,7,9 of continuous respiration segments (i.e., about 3*s*, 9*s*, 15*s*, 21*s*, and 27*s*) to perform the user verification task. We confirm the effectiveness of our majority voting algorithm using multiple respiration segments for testing. For example, the results in Figure 8a show the average verification accuracy increases from around 93.8% to over 96.1%, when we increase

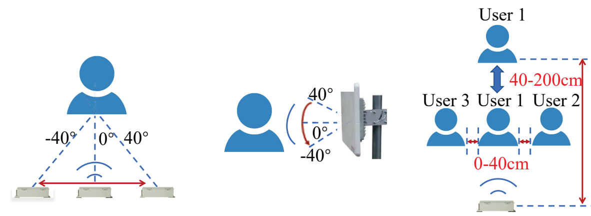

(a) Horizontal orientation (b) Vertical orientation (c) Formation 1 & 2

Figure 10: Illustration of experimental setup for orientation and verifying multiple users.

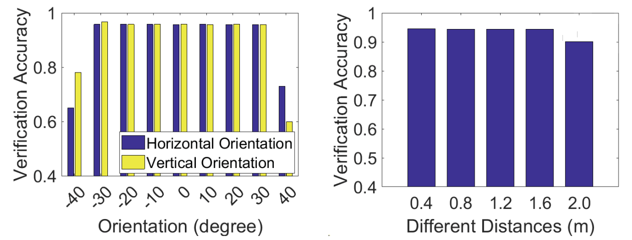

(a) Performance on different orientation (b) Performance on different distances

Figure 11: The impacts of the different orientation and distances.

the number of testing segments from 1 to 9 for the random attack. We also observe that the average verification accuracy increases significantly from 90.1% to 95.3% as the testing segments increase from 1-9 for imitation attack. We have the same observation on the system performance under various attacks as shown in Figure 9a, and Figure 9b. When there are more available testing segments for testing, the ROC curve hugs the point (0,1) more, which indicates the system has better performance on the attack detection.

Impact of Training Size. Since the training data size significantly influences the ease of use in terms of data collection time, we particularly test different training data sizes to evaluate our system. The average verification accuracy of 41 participants shows a growing trend with the increasing training size, which is shown in Figure 8b. In particular, our system achieves an average verification accuracy of 91.6% with 3 training segments. While increasing the number of training segments to 10, the average verification accuracy then grows dramatically to over 93.8%. If we set the training samples to over 20, the system can achieve a comparable verification accuracy of over 95.2%. Moreover, the average verification accuracy becomes stable with 20 to 40 samples. We observe the accuracy gradually drop to 94.7% and 94.1% when using 100 and 200 training segments respectively caused by the overfitting problem. Those results prove that our system is suitable for practical use since it achieves high verification accuracy with limited training segments (e.g., 20 respiration segments per user).

Impact of Tag Orientations. Since the performance of RFID systems is influenced by antenna orientation as well as blockage of line-of-sight paths by the human body, we evaluate the performence at different horizontal and vertical orientations. Figure 10a shows the antenna is moved from left to the right in front of the user horizontally. The angle between the user and attenna is between ±40°. Figure 10b shows we adjust the direction of the antenna at different vertical orientations within ±40°. Figure 11a plots the verification accuracy with different horizontal and vertical orientations. According to the experiment results, when the horizontal

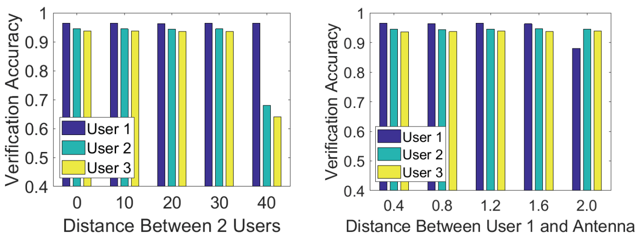

(a) Formation 1 **(b) Formation 2**

Figure 12: Performance comparison for verifying multiple users simultaneously in two formations.

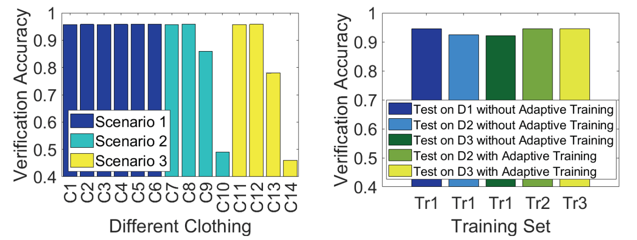

(a) Different clothes **(b) With and without adaptive training**

Figure 13: Performance comparison with different clothes and with/without adaptive training.

and vertical degrees are within the ±30°, the measurement accuracy is around 95.8%. When the orientation is over ±40°, the accuracy decreases to 75.0% − 65.4%, respectively. The reason is that when the orientation exceeds ±40°, the reader can no longer identify the tag or read low-level data.

Impact of Tag-Antenna Distances. We also study the performance of user verification under various distances (i.e., 0.4m to 2.0m) between the target user and the RFID antenna. As shown in Figure 11b, even for the longer distances (i.e., 2.0m), we can still achieve a high verification accuracy of 90.1% using 3 testing respiration segments. We observe that the performance keeps the verification accuracy of 93.9% and 95.2% within the distance of 1.6m with 1 and 3 testing respiration segment(s). The result demonstrates that our system is robust to various distances.

Impact of Multiple Users. We examine the performance of BioTag when multiple people are in the monitoring range of the antenna simultaneously. Particularly, we consider two formations for verifying 3 users with different distances between users as illustrated in Figure 10c: *1) Formation 1:* User 1 is fixed, user 2 and user 3 move away from user 1 with different horizontal distances of 0cm, 10cm, 20cm, 30cm, and 40cm. *2) Formation 2:* User 2 and user 3 are fixed. The horizontal distances between user 1 and user 2, and user 1 and user 3 are 30cm. The vertical distances between user 1 and the antenna is 40cm, 80cm, 120m, 160m and 200cm. Figure 12a shows that BioTag maintains a similarly high accuracy (i.e., 96.4%, 94.5%, and 93.3%) for the three users in Formation 1 when the distances between them are less than 30cm. The accuracy of user 2 and 3 degrade to around 60.2% when the distance is over 30cm, indicating the users are out of the monitoring range. Figure 12b shows that the accuracy of three users in Formation 2 keeps the same when the distance between user 1 and the antenna is less than 1.6m. When the distance is over 1.6m, the accuracy of user 1 drops to 88.4%, and the other two users still keep the similar accuracy, indicating BioTag can efficiently distinguish the multiple users simultaneously as long as they are within the monitoring range (i.e., 1.6m).

Impact of Clothes. We design 3 scenarios to evaluate the impact of different layers of clothes and materials on our performance. Specifically, *1) Scenario 1:* C1-C6 denote the users wearing one layer of clothes made from different materials (i.e., underwear (94% cotton, 6% polyester), T-shirt (100% cotton), shirt (100% cotton), sweater-1 (100% polyester), sweater-2 (100% cotton), jacket(100% polyester + 100% cotton)) with the tags on the clothes. *2) Scenario 2:* C7-C10 denote the users wearing two layers of clothes (i.e., underwear with shirt, T-shirt with sweater-1, shirt with sweater-1, and shirt with down jacket) with the tags on the outer-layer clothes. *3) Scenario 3:* C11-C14 denote the users wearing the same clothes as C7-C10 but with two tags attached between two layers of the clothes. Figure 13a shows that we can achieve over 95.9% verification accuracy when the users wear one layer of clothes regardless of the materials. In Scenario 2 and Scenario 3, we can observe that the average verification accuracy drops with the increasing clothes' thickness in a range of 95.8% − 58.6%. This is mainly because thick clothes block RFID, resulting in smaller signal-to-noise-ratio. In addition, thick clothes are usually too stiff to move with respiration.

Effectiveness of Adaptive Training. We evaluate our adaptive training using the data collected by 28 of 41 users across three different days in the same hours (i.e., $1 - 3PM$). In Figure 13b, $Tr1$ represents the training set is only from day 1. $Tr2$ and $Tr3$ represent the mixed training set, including the data from both day 1 + day 2 and day 1 + day 3, respectively. We can see that our system trained by $Tr1$ can achieve 94.6% accuracy during day 1, and decrease 5% during day 2 and 6% during day 3, respectively. These results demonstrate that the respiratory pattern has some fluctuations over time due to participants' status (e.g., pain, body temperature, body position) that slightly impact the system performance. The figure shows that after applying the adaptive training using the data from $Tr2$ and $Tr3$, the accuracy increases to 94.5% and 94.6% on day 2 and day 3, respectively. Those results prove that our system is suitable for continuous user verification with few times of adaptively retraining on a very small amount of new data (i.e., a routine retrain every 3 hours with only 1-min new data).

7 DISCUSSION

1. Respiratory Pattern Dynamics. We find vigorous exercise would significantly affect the respiratory patterns in terms of morphological characteristics, leading to changes in fiducial features and failures in our system. Such cases can be addressed by asking users to wait for a short time (e.g., 3mins) until their respiration become normal. It is also possible to train a model using the users' data collected during the exercise recovering period to enable continuous user verification under normal or after exercises. **2. Environmental Dynamics.** We find RFID signals are susceptible to dynamic environmental changes (e.g., people walking around). Since the normal breathing frequency is in the range of 0.2 − 0.3 Hz and the typical bandwidth of normal human gestures is between 4 and 6 Hz, adopting a low-pass filter could be a potential way of effectively mitigating such impacts. As for other human daily activities, their frequency [10] resides in the range between 0 and 20 Hz. Therefore, we can use advanced signal processing techniques (e.g., empirical mode decomposition) to filter out noises with overlapping frequencies as human respiration. **3. Body Movements and Emotions.** Our experiments are conducted with participants sitting on a chair to keep their bodies stable with normal emotions. We find that the participants experience some nonspontaneous body movements (e.g., body moving back and forth) when they conduct the experiments standing. Furthermore, the various emotions (e.g., anxiety and excitement) also impact the respiratory pattern. Therefore, we plan to explore additional tags at different positions and deep-learning-based user motion mitigation methods in our future work to remove the impacts of nonspontaneous body movements. We also plan to examine the impact of user emotion and improve the robustness and accuracy of our system in realistic environments.

8 CONCLUSION

We propose BioTag, a continuous user verification system that can identify legitimate users by leveraging the physiological features of respirator patterns captured by commodity low-cost RFID devices. In this work, we extensively explore and identify the effective locations on human bodies for capturing unique holistic respiratory characteristics using RFID tags. We develop unique respiratory features based on waveform morphology analysis and fuzzy wavelet transformation. We also design an adaptive GBDT classifier that accurately identifies legitimate users and attackers. Extensive experiments involving 41 participants demonstrate that the proposed system robustly verifies users' identities and detects attackers under random and imitation attacks with only a little training effort.

ACKNOWLEDGMENT

This work was partially supported by the the National Science Foundation Grants CCF2028873, CCF1909963, CNS2120350, CNS2120396, CCF2000480, CNS2120276, and CNS2145389.

REFERENCES

[1] Fadel Adib, Hongzi Mao, Zachary Kabelac, Dina Katabi, and Robert C Miller. 2015. Smart homes that monitor breathing and heart rate. In *Proceedings of the 33rd annual ACM conference on human factors in computing systems*. 837–846.

[2] Adam J Aviv, Katherine L Gibson, Evan Mossop, Matt Blaze, and Jonathan M Smith. 2010. Smudge attacks on smartphone touch screens. *Woot* 10 (2010), 1–7.

[3] Sheldon R Braun. 1990. Respiratory rate and pattern. *Clinical Methods: The History, Physical, and Laboratory Examinations. 3rd edition* (1990).

[4] Lars Buitinck, Gilles Louppe, Mathieu Blondel, Fabian Pedregosa, Andreas Mueller, Olivier Grisel, Vlad Niculae, Peter Prettenhofer, Alexandre Gramfort, Jaques Grobler, Robert Layton, Jake VanderPlas, Arnaud Joly, Brian Holt, and Gaël Varoquaux. 2013. API design for machine learning software: experiences from the scikit-learn project. In *ECML PKDD Workshop: Languages for Data Mining and Machine Learning*. 108–122.

[5] Jagmohan Chauhan, Yining Hu, Suranga Seneviratne, Archan Misra, Aruna Seneviratne, and Youngki Lee. 2017. BreathPrint: Breathing acoustics-based user authentication. In *Proceedings of the 15th Annual International Conference on Mobile Systems, Applications, and Services*. 278–291.

[6] Jerome H Friedman. 2001. Greedy function approximation: a gradient boosting machine. *Annals of statistics* (2001), 1189–1232.

[7] Anna Huang, Dong Wang, Run Zhao, and Qian Zhang. 2019. Au-id: Automatic user identification and authentication through the motions captured from sequential human activities using rfid. *Proceedings of the ACM on Interactive, Mobile, Wearable and Ubiquitous Technologies* 3, 2 (2019), 1–26.

[8] Espen Alexander Fürst EAFI Ihlen. 2012. Introduction to multifractal detrended fluctuation analysis in Matlab. *Frontiers in physiology* 3 (2012), 141.

[9] Nima Karimian, Mark Tehranipoor, and Domenic Forte. 2017. Non-fiducial ppg-based authentication for healthcare application. In *2017 IEEE EMBS international conference on biomedical & health informatics (BHI)*. IEEE, 429–432.

[10] Rinat Khusainov, Djamel Azzi, Ifeyinwa E Achumba, and Sebastian D Bersch. 2013. Real-time human ambulation, activity, and physiological monitoring: Taxonomy of issues, techniques, applications, challenges and limitations. *Sensors* 13, 10 (2013), 12852–12902.

[11] Rami N Khushaba, Sarath Kodagoda, Sara Lal, and Gamini Dissanayake. 2010. Driver drowsiness classification using fuzzy wavelet-packet-based feature-extraction algorithm. *IEEE transactions on biomedical engineering* 58, 1 (2010), 121–131.

[12] Arash Habibi Lashkari, Samaneh Farmand, Dr Zakaria, Omar Bin, Dr Saleh, et al. 2009. Shoulder surfing attack in graphical password authentication. *arXiv preprint arXiv:0912.0951* (2009).

[13] Feng Lin, Chen Song, Yan Zhuang, Wenyao Xu, Changzhi Li, and Kui Ren. 2017. Cardiac scan: A non-contact and continuous heart-based user authentication system. In *Proceedings of the 23rd Annual International Conference on Mobile Computing and Networking*. 315–328.

[14] Jian Liu, Yingying Chen, Yudi Dong, Yan Wang, Tiannming Zhao, and Yu-Dong Yao. 2020. Continuous user verification via respiratory biometrics. In *IEEE INFOCOM 2020-IEEE Conference on Computer Communications*. IEEE, 1–10.

[15] Shrirang Mare, Andrés Molina Markham, Cory Cornelius, Ronald Peterson, and David Kotz. 2014. Zebra: Zero-effort bilateral recurring authentication. In *2014 IEEE Symposium on Security and Privacy*. IEEE, 705–720.

[16] Sky McKinley and Megan Levine. 1998. Cubic spline interpolation. *College of the Redwoods* 45, 1 (1998), 1049–1060.

[17] Gilad Mishne. 2006. Autotag: a collaborative approach to automated tag assignment for weblog posts. In *Proceedings of the 15th international conference on World Wide Web*. 953–954.

[18] Meinard Müller. 2007. Dynamic time warping. *Information retrieval for music and motion* (2007), 69–84.

[19] Jingyi Ning, Lei Xie, Chuyu Wang, Yanling Bu, Fengyuan Xu, Da-Wei Zhou, Sanglu Lu, and Baoliu Ye. 2021. RF-Badge: Vital Sign-based Authentication via RFID Tag Array on Badges. *IEEE Transactions on Mobile Computing* (2021).

[20] Verônica F Parreira, Carolina J Bueno, Danielle C França, Danielle SR Vieira, Dirceu R Pereira, and Raquel R Britto. 2010. Breathing pattern and thoracoabdominal motion in healthy individuals: influence of age and sex. *Brazilian Journal of Physical Therapy* 14 (2010), 411–416.

[21] Konstantinos N Plataniotis, Dimitrios Hatzinakos, and Jimmy KM Lee. 2006. ECG biometric recognition without fiducial detection. In *2006 Biometrics symposium: Special session on research at the biometric consortium conference*. IEEE, 1–6.

[22] Maria Ragnarsdóttir and Ella Kolbrun Kristinsdóttir. 2006. Breathing movements and breathing patterns among healthy men and women 20–69 years of age. *Respiration* 73, 1 (2006), 48–54.

[23] Mark Roberti. 2004. EPCglobal ratifies Gen 2 standard. *RFID Journal* 16 (2004).

[24] Roger P Simon, Michael Jeffrey Aminoff, David A Greenberg, et al. 2009. *Clinical neurology*. Lange Medical Books/McGraw-Hill.

[25] Issa Traore, Isaac Woungang, Mohammad S Obaidat, Youssef Nakkabi, and Iris Lai. 2012. Combining mouse and keystroke dynamics biometrics for risk-based authentication in web environments. In *2012 fourth international conference on digital home*. IEEE, 138–145.

[26] Aggeliki Tsoli, Naureen Mahmood, and Michael J Black. 2014. Breathing life into shape: Capturing, modeling and animating 3D human breathing. *ACM Transactions on graphics (TOG)* 33, 4 (2014), 1–11.

[27] Chuyu Wang, Lei Xie, Wei Wang, Yingying Chen, Yanling Bu, and Sanglu Lu. 2018. Rf-ecg: Heart rate variability assessment based on cots rfid tag array. *Proceedings of the ACM on Interactive, Mobile, Wearable and Ubiquitous Technologies* 2, 2 (2018), 1–26.

[28] Fei Wang, Zhenjiang Li, and Jinsong Han. 2019. Continuous user authentication by contactless wireless sensing. *IEEE Internet of Things Journal* 6, 5 (2019), 8323–8331.

[29] Yanwen Wang and Yuanqing Zheng. 2019. TagBreathe: Monitor breathing with commodity RFID systems. *IEEE Transactions on Mobile Computing* 19, 4 (2019), 969–981.

[30] Greg Welch, Gary Bishop, et al. 1995. An introduction to the Kalman filter. (1995).

[31] Weiye Xu, Jianwei Liu, Shimin Zhang, Yuanqing Zheng, Feng Lin, Jinsong Han, Fu Xiao, and Kui Ren. 2021. RFace: anti-spoofing facial authentication using cots rfid. In *IEEE INFOCOM 2021-IEEE Conference on Computer Communications*. IEEE, 1–10.

[32] Chao Yang, Xuyu Wang, and Shiwen Mao. 2018. AutoTag: Recurrent variational autoencoder for unsupervised apnea detection with RFID tags. In *2018 IEEE Global Communications Conference (GLOBECOM)*. IEEE, 1–7.

[33] Lei Yang, Yekui Chen, Xiang-Yang Li, Chaowei Xiao, Mo Li, and Yunhao Liu. 2014. Tagoram: Real-time tracking of mobile RFID tags to high precision using COTS devices. In *Proceedings of the 20th annual international conference on Mobile computing and networking*. 237–248.

[34] Yunze Zeng, Parth H Pathak, and Prasant Mohapatra. 2016. WiWho: WiFi-based person identification in smart spaces. In *2016 15th ACM/IEEE International Conference on Information Processing in Sensor Networks (IPSN)*. IEEE, 1–12.

[35] Shigeng Zhang, Xuan Liu, Yangyang Liu, Bo Ding, Song Guo, and Jianxin Wang. 2020. Accurate respiration monitoring for mobile users with commercial RFID devices. *IEEE Journal on Selected Areas in Communications* 39, 2 (2020), 513–525.

[36] Tianming Zhao, Yan Wang, Jian Liu, Yingying Chen, Jerry Cheng, and Jiadi Yu. 2020. Trueheart: Continuous authentication on wrist-worn wearables using ppg-based biometrics. In *IEEE INFOCOM 2020-IEEE Conference on Computer Communications*. IEEE, 30–39.